J|A|C|S
COMMUNICATIONS

Published on Web 02/14/2006

Effects of Solvent Viscosity on Ligand Interconversion Dynamics in the Primary Docking Site of Heme Proteins

Seongheun Kim, Jeonghee Heo, and Manho Lim*

Department of Chemistry, Pusan National University, Busan 609-735, Korea

Received December 2, 2005; E-mail: mhlim@pusan.ac.kr

Protein structural dynamics plays a significant role in the control of protein reactivity and thus its function. One prominent example is that conformational relaxation of myoglobin (Mb) and hemoglobin (Hb) after deligation slows the rate of ligand rebinding.[1−4] Protein undergoes a broad range of structural fluctuation including a large-amplitude collective motion as well as a smaller and more local internal motion. Delineating which and how global motion of a protein is coupled to functionally important internal motions of the protein is essential to understand biomechanics of protein.[2,5] One way of studying the coupling between various protein dynamics is to influence protein surface motions, which can substantially affect its internal structural dynamics, by varying the solvent viscosity and monitor the alteration in dynamics.[3,4,6] Glycerol has been extensively employed as a viscogenic cosolvent to vary solvent viscosity[7,8] and a glass-forming dried trehalose as an effectively infinite viscosity solvent.[3,4,8,9] The trehalose glass matrix locks the surface of protein, thereby selectively eliminating the large-amplitude solvent-coupled protein fluctuations and cooperative relaxation modes and leaving only side-chain motions and local relaxation modes.[9,10] Interconversion among taxonomic conformational substates (*A*-states) of MbCO, the escape of CO from the heme pocket, and conformational relaxation of the protein are severely hindered in trehalose glass.[3,4,9] The average geminate rebinding rates in the glass are much higher than those in aqueous solution due to retardation of the structural relaxation of the protein that raises the average energy barrier for the ligand binding.[3,4] The vibrational dephasing of bound CO is significantly slower for Mb and Hb embedded in trehalose glasses compared to that of aqueous protein solutions.[11]

Recently, we have measured interconversion dynamics of the ligand in the primary docking site (PDS) of heme proteins[12] located on top of the heme group about 2 Å from the active binding site[13,14] and known to modulate ligand-binding activity by mediating the passage of ligand to and from the active binding site.[14,15] Ligands in two states of the PDS interconvert on the picosecond time scale, and the rates are about 4 times slower in Hb than Mb.[12] Here we extend our early investigation and study the interconversion dynamics of the ligand in the PDS of Mb and Hb in viscous solvents to elucidate the extent of the coupling between the functionally important protein internal dynamics and the solvent-coupled large-scale protein motion.

Absorption spectra of the stretching mode of CO photolyzed from and bound to Mb and Hb in various solvents are shown in Figure 1 (experimental methods are provided in the Supporting Information). Solvent modifies the resonance frequencies of the vibrational bands and the partitioning between different taxonomic structural substates of the proteins. The modification in bound CO spectra was suggested to arise from the difference of the potential energy surface of the proteins.[8] Time evolution of the vibrational bands of CO photolyzed from MbCO and HbCO in trehalose at 283 K is shown in Figure 2.[17] The spectral features are very similar to those

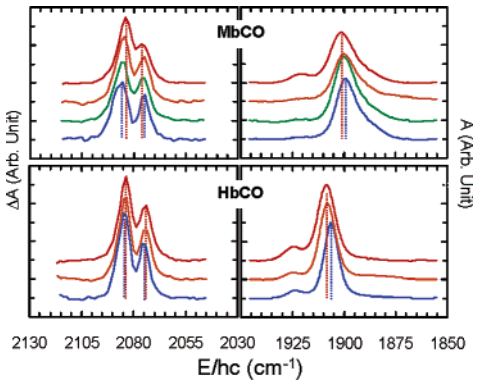

Figure 1. Normalized and background subtracted IR absorption spectra of the stretching mode of ^{13}CO photolyzed from (left, *B*-state) and bound to (right, *A*-state) Mb and Hb in D_2O (blue), 65 wt % glycerol/D_2O (green), 75 wt % glycerol/D_2O (orange), and trehalose (red). The color-coded dotted vertical lines are shown to indicate center wavenumber of each band. Spectra of *B*-state are obtained at 100 ps after photolysis of CO-ligated proteins, and those of *A*-state are equilibrium spectra.

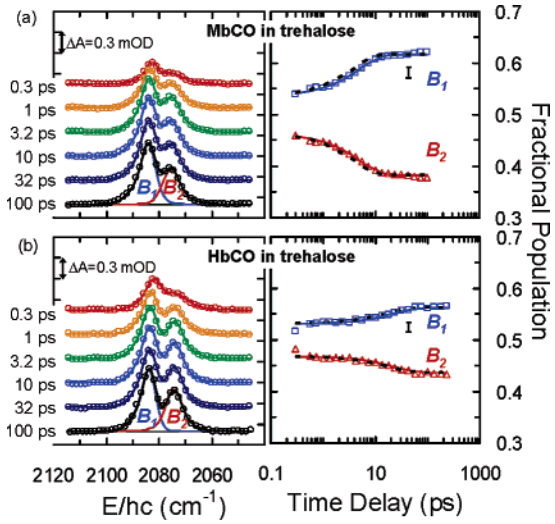

Figure 2. Left: Representative time-resolved vibrational spectra of ^{13}CO photolyzed from Mb^{13}CO (a) and Hb^{13}CO (b) in trehalose at 283K. The data (○) are fit to two evolving bands (B_1 and B_2) (—).[16] Right: Time evolution of the fractional population of each band of photolyzed MbCO and HbCO. The data (□, △) are fit to a two-states model approaching equilibrium (—).[12] Error bars are shown to indicate reproducibility of the data. For comparison, $f_i(t)$ in D_2O was calculated by incorporating values of $f_i(0)$ and k_{21}/k_{12} in trehalose into k in D_2O (thick dashed black lines).

in D_2O,[12,16] in that the spectral intensity initially grows due to protein rearrangement[14] and the bands shift and narrow due to conformational relaxation of the protein.[16] The two bands arise from CO located in the PDS with opposite orientations after photolysis from the protein.[14,15,18] Since the deligated CO neither rebinds nor escapes from the PDS during the present experimental time window of <300 ps,[19] CO population in the PDS remains constant after its

10.1021/ja058201w CCC: $33.50

Table 1. Least-Squares Fit Parameters Obtained by Modeling the Fractional Population and Calculated Thermochemical Values at 283 K Using the Parameters[12]

sample	solvent	$1/k_{12}$ (ps)	$1/k_{21}$ (ps)	$f_1(0)$	ΔG^a (kJ/mol)	$E_{\alpha 21}{}^{max\ b}$ (kJ/mol)
MbCO						
	D_2O[12]	10 ± 0.5	6 ± 0.4	0.50 ± 0.02	1.2 ± 0.1	7.5 ± 0.2
	65:35 G/W	10 ± 1	6.5 ± 1	0.52 ± 0.03	1.0 ± 0.1	7.7 ± 0.4
	75:25 G/W	14 ± 2	9 ± 1	0.54 ± 0.03	1.0 ± 0.1	8.4 ± 0.3
	trehalose	13 ± 2	8 ± 1	0.54 ± 0.03	1.1 ± 0.1	8.2 ± 0.3
HbCO						
	D_2O[12]	43 ± 2	26 ± 1	0.56 ± 0.02	1.2 ± 0.1	10.9 ± 0.1
	75:25 G/W	51 ± 8	33 ± 6	0.57 ± 0.03	1.0 ± 0.1	11.5 ± 0.5
	trehalose	53 ± 11	41 ± 7	0.53 ± 0.03	0.6 ± 0.1	12 ± 0.4

[a] The difference free energy, $\Delta G = G(B_2) - G(B_1) = -RT \ln(k_{21}/k_{12})$. [b] The maximum possible rotational barrier from B_2 to B_1, $E_{\alpha 21}{}^{max}$ was calculated assuming that the fastest attempt frequency for crossing the barrier is $(0.25\ ps)^{-1}$, the inverse time for gas-phase CO to rotate 90° at 283 K.[12,18]

establishment with a subpicosecond time scale.[14] While total population of CO in the PDS is maintained constant, the fractional population of each band evolves in time (see Figure 2). Evidently, the nascent distribution of photoproduct in each state is not in thermal equilibrium, but approaches equilibrium, from which interconversion dynamics between two bands can be extracted. The time evolution has been described by a two-state (B_1 and B_2) model proceeding toward equilibrium with rate constants of k_{12} and k_{21}, where k_{ij} is the rate constant from B_i to B_j. In this model, time-dependent fractional population of B_i, $f_i(t)$ is expressed by $f_i(t) = k_{ji}/k + (f_i(0) - k_{ji}/k) \exp(-kt)$, where $k = k_{12} + k_{21}$.[12]

The least-squares fit parameters obtained by fitting $f_i(t)$ of Mb and Hb in various solvents and their calculated thermochemical values at 283 K from the parameters are summarized in Table 1. The nascent yields of B_1 after photolysis in both proteins appear to be within experimental scatter, but they may be slightly higher in Hb.[12] The interconversion rates in the viscous solutions may be slower than those in the aqueous solution. However, within experimental error, the difference is negligible; $f_i(t)$ in D_2O is well overlapped with that in viscous solvents (thick dashed black lines in Figure 2). Apparently the interconversion dynamics is minimally coupled to dynamics in the protein's surface topology changes of which require motions of the solvent. If the interconversion barrier is not altered by conformational relaxation of the protein at all or if the interconversion barrier in the PDS is established within a few picoseconds after photolysis and weakly coupled to the slow global conformational relaxation, internal dynamics of the ligand in the PDS will negligibly depend on solvent viscosity as observed here. As manifested in the initial growth of the integrated area of the absorption band,[12,14,16] protein rearranges to constrain the orientation of docked CO after photolysis.[14] Thus, the interconversion barrier is likely modified by the conformational change of the protein. The major proximal relaxation occurs on the picosecond time scale even in viscous solution.[4,10,20] Consequently, the major proximal relaxation as well as fast distal relaxation may be the dominant factor establishing the interconversion barrier.

The lack of viscosity dependence in the interconversion dynamics is consistent with findings of a recent analysis of geminate CO rebinding in Mb using a modified Agmon Hopfield model.[10,21] The analysis reveals a hierarchy of functionally important protein dynamics that shows varying degrees of coupling to the solvent under high viscosity conditions.[10] Among several distal pocket modes controlling the rebinding kinetics, the distal histidine mode is not slaved to the solvent.[10] Clearly, there are dynamics that influence CO rebinding to Mb that are negligibly coupled to the solvent. This category of dynamics should be responsible for protein motions needed to establish the ligand interconversion barrier in the PDS. In addition, in contrast to ligand diffusion among the internal pockets that requires large local motion of the protein,[10] ligand interconversion within the PDS should require, if any, only small amplitude side-chain motions isolated from the solvent in the interior of the protein.

The difference free energy between *B* states of Hb is strongly influenced by solvent, while that of Mb is not. The quaternary structure may cause the solvent effect on the PDS to be more important thermodynamically than kinetically. Interconversion rates in the PDS of Hb in water solution are slower than those of Mb in trehalose, indicating that the interconversion barrier in Hb is intrinsically higher than that in Mb and is not modified by the solvent viscosity. The quaternary contact likely plays a much greater role in the interconversion dynamics than the protein's surface topology.

Acknowledgment. This work was supported by the SRC program of MOST/KOSEF (R11-2000-070-04004-0) and the KRF Grant funded by the Korean Government (MOEHRD) (KRF-2005-070-C00063).

Supporting Information Available: Experimental procedures. This material is available free of charge via the Internet at http://pubs.acs.org.

References

(1) Austin, R. H.; Beeson, K. W.; Eisenstein, L.; Frauenfelder, H.; Gunsalus, I. C. *Biochemistry* **1975**, *14*, 5355−5373.
(2) Ansari, A.; Berendzen, J.; Braunstein, D. K.; Cowen, B. R.; Frauenfelder, H.; Hong, M. K.; Iben, I. E. T.; Johnson, J. B.; Ormos, P.; Sauke, T. B.; Scholl, R.; Schulte, A.; Steinbach, P. J.; Vittitow, J.; Young, R. D. *Biophys. Chem.* **1987**, *26*, 337−355.
(3) Hagen, S. J.; Hofrichter, J.; Eaton, W. A. *J. Phys. Chem.* **1996**, *100*, 12008−12021.
(4) Gottfried, D. S.; Peterson, E. S.; Sheikh, A. G.; Wang, J.; Yang, M.; Friedman, J. M. *J. Phys. Chem.* **1996**, *100*, 12034−12042.
(5) Vitkup, D.; Ringe, D.; Petsko, G. A.; Karplus, M. *Nat. Struct. Biol.* **2000**, *7*, 34−38.
(6) Beece, D.; Eisenstein, L.; Frauenfelder, H.; Good, D.; Marden, M. C.; Reinisch, L.; Reynolds, A. H.; Sorensen, L. B.; Yue, K. T. *Biochemistry* **1980**, *19*, 5147−5157.
(7) Ansari, A.; Jones, C. M.; Henry, E. R.; Hofrichter, J.; Eaton, W. A. *Science* **1992**, *256*, 1796−1798.
(8) McClain, B. L.; Finkelstein, I. J.; Fayer, M. D. *J. Am. Chem. Soc.* **2004**, *126*, 15702−15710.
(9) Librizzi, F.; Viappiani, C.; Abbruzzetti, S.; Cordone, L. *J. Chem. Phys.* **2002**, *116*, 1193−1200.
(10) Dantsker, D.; Samuni, U.; Friedman, J. M.; Agmon, N. *Biochim. Biophys. Acta* **2005**, *1749*, 234−251.
(11) Massari, A. M.; Finkelstein, I. J.; McClain, B. L.; Goj, A.; Wen, X.; Bren, K. L.; Loring, R. F.; Fayer, M. D. *J. Am. Chem. Soc.* **2005**, *127*, 14279−14289.
(12) Kim, S.; Lim, M. *J. Am. Chem. Soc.* **2005**, *127*, 5786−5787.
(13) (a) Schlichting, I.; Berendzen, J.; Phillips, G. N., Jr.; Sweet, R. M. *Nature* **1994**, *371*, 808−812. (b) Teng, T. Y.; Srajer, V.; Moffat, K. *Nat. Struct. Biol.* **1994**, *1*, 701−705.
(14) Lim, M.; Jackson, T. A.; Anfinrud, P. A. *Nat. Struct. Biol.* **1997**, *4*, 209−214.
(15) Lim, M.; Jackson, T. A.; Anfinrud, P. A. *J. Am. Chem. Soc.* **2004**, *126*, 7946−7957.
(16) Kim, S.; Heo, J.; Lim, M. *Bull. Korean Chem. Soc.* **2005**, *26*, 151−156.
(17) Two features are apparent at 0.3 ps and fully developed in <1 ps, consistent with ultrafast photolysis of CO from the protein and the suggestion that CO is funneled into the PDS.[14,15] To characterize the spectral evolution, absorption features were fit to two evolving bands (B_1 and B_2), and each band is modeled with a sum of two Gaussians on a cubic polynomial background.[15,16,18] The single feature consisting of a sum of two Gaussians depicts an asymmetric band, which likely arises from an anisotropic spatial distribution of photolyzed CO and/or conformational substates of protein.[15,16,18] The total integrated area grows with a time constant of 1.1 ± 0.1 ps.
(18) Lim, M.; Jackson, T. A.; Anfinrud, P. A. *J. Chem. Phys.* **1995**, *102*, 4355−4366.
(19) (a) Henry, E. R.; Sommer, J. H.; Hofrichter, J.; Eaton, W. A. *J. Mol. Biol.* **1983**, *166*, 443−451. (b) Murray, L. P.; Hofrichter, J.; Henry, E. R.; Eaton, W. A. *Biophys. Chem.* **1988**, *29*, 63−76.
(20) Lim, M.; Jackson, T. A.; Anfinrud, P. A. *Proc. Natl. Acad. Sci. U.S.A.* **1993**, *90*, 5801−5804.
(21) Dantsker, D.; Roche, C.; Samuni, U.; Blouin, G.; Olson, J. S.; Friedman, J. M. *J. Biol. Chem.* **2005**, *280*, 38740−38755.

JA058201W